MOCVD Growth of Strained Multiple Quantum Well Structure for 1.3 μm InAsP/InP Laser Diodes

Chong-Yi Lee(李重義), Meng-Chyi Wu(吳孟奇), Hung-Pin Shiao[a)](蕭宏彬), Tian-Tsorng Shi[a)](施天從), and Wen-Jeng Ho[a)](何文章)

Research Institute of Electrical Engineering, National Tsing Hua University, Hsinchu 300, Taiwan, Republic of China
Tel: +886-3-5715131-4038
Fax: +886-3-5715971
e-mail address: mcwu@ee.nthu.edu.tw

[a)] Photonic Technology Research, Telecommunication Laboratories, Ministry of Transportation and Communications, Yang-Mei 326, Taiwan, Republic of China

計劃名稱: 1.3μm波長GaInP/InAsP/InP雷射二極體之研究
計劃編號: NSC88-2215-E-007-004
執行期限: 87.8.1~88.7.31

主持人: 吳孟奇　　　　國立清華大學電機工程研究所

Strained multiple quantum wells (SMQWs) have attracted considerable attention. The biaxial strain incorporated into the quantum wells by an intentional lattice mismatch causes the reduction of in-plane Hall effective mass and thus reduces the valence-band density of states [1,2]. Therefore, population inversion of the laser diodes (LDs) occurs at low injection carrier densities, which result in a lowering at threshold current [3]. The altered valence band-band structure also suppresses the inter-valence band absorption and the Auger recombination [1].

For the active-layer material in these SMQWs, compressively strained GaInAs, GaInAsP and AlGaInAs were used exclusively. InAsP system on InP substrates could be suitable for compressively strained quantum well in all the range of alloy composition, covering a luminescence bandgap in the wavelength range of 1.0 to 3.0 μm. In addition, InAsP has the added benefit of a large conduction-band offset, $\Delta E_C = 0.7\ \Delta E_g$ [4,5], as compared to GaInAs/InP or GaInAsP/InP ($\Delta E_C = 0.4\ \Delta E_g$). Yamada *et al.* reported a compressive InAsP SMQW laser exhibiting a characteristic temperature, To, as high as 143 K [6]. Strain compensation using tensile-strained barriers has been adopted to counter-balance the compressive strain induced by InAsP well. Tensile-strained GaInP, GaInAsP and AlGaInAs barriers have been incorporated. However, the report on growing InAsP/InP SMQWs without compensative barriers at lower temperatures by MOCVD is still lacking. Better understanding of this low-temperature growth for the strain-uncompensated InAsP/InP SMQW structures would be helpful in the optoelectronic device development.

In this study, the epitaxial layers of InAsP/InP SCH-SMQW LDs grown on a (100) oriented S-doped n-InP substrate consisted of:

i) n-InP buffer layer (0.6 μm thick; $1\text{x}10^{18}$ cm^{-3})

ii) undoped GaInAsP SCH layer ($\lambda_g = 1.1$ μm; 100 nm thick)

iii) active region composed of five or three periods of $InAs_{0.5}P_{0.5}$ (3.6 nm thick) / InP (14.4 nm thick) SMQWs sandwiched by undoped InP layer (15 nm thick)

iv) undoped GaInAsP SCH layer (λ_g = 1.1 μm; 100 nm thick)

v) p-InP cladding layer (1.5 μm thick; 1×10^{18} cm^{-3})

vi) p^+-GaInAs contact layer (0.2 μm thick; 2×10^{19} cm^{-3}).

Uncoated 50-μm width broad-area (BA) LDs with a cavity length (L) ranging from 300 to 900 μm and 2-μm width ridge waveguide (RWG) LDs with a cavity length of 300 μm were fabricated using standard photolithography techniques. The Ti/Pt/Au contact metal was deposited on the top of the GaInAs contact layer and the backside of the polished substrate. Finally, rapid thermal annealing (RTA) for 25 s at 420 °C and 500 °C were applied to the samples of BA and RWG LDs, respectively.

A typical light-current (L-I) characteristic and slope efficiency curves for BA LDs with different cavity lengths are shown in Fig.1. The inset in Fig.1 shows the amplitude simulation for the fields propagated out of this thin-film waveguide with 300 μm cavity length by beam-propagation method. The threshold current and slope efficiency for the 300, 600 and 900-μm cavity length LDs was 942, 1062 and 1222 mA and 0.048, 0.037 and 0.025, respectively.

Threshold current density (J_{th}) of BA LDs versus cavity length is shown in Fig.2. Assuming nonlinear gain in the logarithmic form, the threshold current density is given as follow:

$$J_{th} = \frac{N_w J_0}{\eta_i} \exp\left(\frac{\alpha_i + (1/L)\ln(1/R)}{N_w \Gamma_w G_0}\right) \quad (1)$$

where N_w is the number of wells, J_0 is the transparency current density, G_0 is the gain coefficient, Γ_w is the optical confinement factor per well, α_i is the internal loss, η_i is the internal quantum efficiency, R is the facet reflectivity and L is the cavity length. α_i is estimated to be 61.9 (η_i = 25.1 %) and 52.7 cm^{-1} (η_i = 24.1 %) for the three-well and five-well SMQW-BA LDs from the measurement of the inverse differential quantum efficiency as a function of cavity length, respectively. $N_w\Gamma_w$ of three-well and five-well SMQW-BA LDs is calculated to be 0.0172 and 0.0285, respectively. By fitting the curve given in Eq.(1) to experimental data points, we get G_0 = 1750 and 1083 cm^{-1} and J_0 = 23.3 and 16.2 A/cm^2 for three-well and five-well SMQW-BA LDs, respectively. These values are not comparable to previous reports of typical SMQW LDs. However, room-temperature lasing spectrum of a 50 x 600 μm^2 as-cleaved BA LD, as shown in Fig.3, is still in a good agreement with our design. The lasing wavelength is 1.261 μm. The inset shows the lasing wavelength as a function of cavity length.

Light output power versus injected current characteristic and longitudinal-mode spectra of a 2 x 300 μm^2 as-cleaved RWG LD under room-temperature pulsed operation are shown in Fig.4. Threshold current is 78.8 mA. All the lasing peak wavelengths locate around 1.24 μm and slightly shift to shorter wavelengths as well as more modes generated with increasing injection current. This is due to the band-filling behavior that leads to laser modes at higher energies.

In conclusion, we have investigated the growth and characterization for the InAsP/InP SCH-SMQW LDs grown at 580 °C. Although laser emission is achieved by using the InAsP/InP SMQWs as the active layer and lasing spectra are in a good

agreement with our design, the active region dislocations will degrade the LD performance. To improve the characteristics of InAsP/InP SMQW LDs for 1.3 μm emission wavelength, tensile-strained barrier material must be employed to compensate the compressive strain in the InAsP well.

The financial support from National Science Council (**NSC 88-2215-E-007-004**) and Photonic Technology Research, Telecommunication Laboratories, Chunghwa Telecom Co., is deeply appreciated.

Reference:

[1] Adams, A. R., *Electron. Lett.*, 1986, **22,** p.249.
[2] Yablonovitch, E., and Kane, E. O., *J. Lightwave Technol.*, 1988, **6,** p.1292.
[3] Yablonovitch, E., and Kane, E. O., *J. Lightwave Technol.*, 1986, **4,** p.504.
[4] Schneider, R. P., Wessels, J., and Wessels, B. W., *J. Electron. Mater.*, 1991, **20,** p.1117.
[5] Monier, C., Vilela, M. F., Serdiukova, I., and Freundlich, A., *Appl. Phys. Lett.*, 1998, **72,** p.1587.
[6] Yamada, M., Anan, T., Tokutome, K., and Sugou, S., *IEEE Photon. Tech. Lett.*, 1999, **11,** p.164.

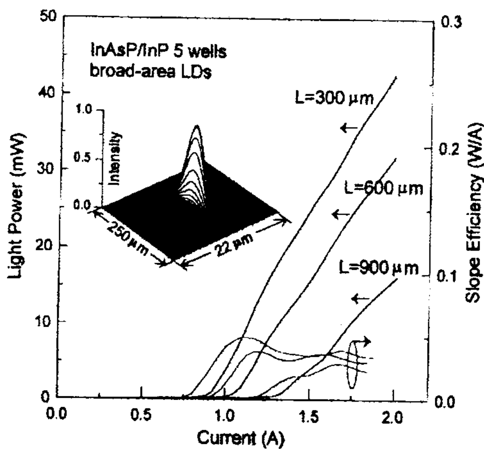

Fig.1 Pulsed light-current characteristics and slope efficiency curves for 50-μm wide as-cleaved BA LDs with different cavity lengths. The amplitude simulation for the fields propagated out of this thin-film waveguide with 300 μm cavity length by beam-propagation method is also shown in the inset.

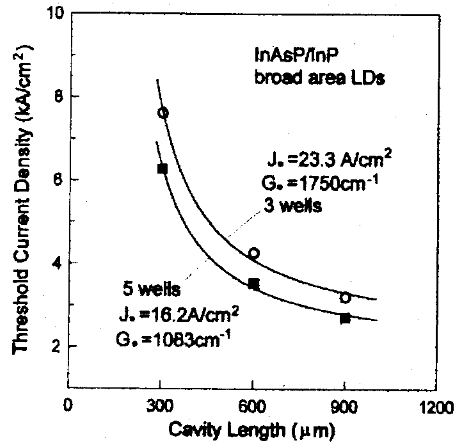

Fig.2 Threshold current density versus cavity length for 50-μm wide as cleaved BA LDs. The calculated curve is also shown. The fitting parameters are J_0 = 23.3 and 16.2 A/cm^2 and G_0 = 1750 and 1083 cm^{-1} for three-well and five-well SMQW lasers, respectively.

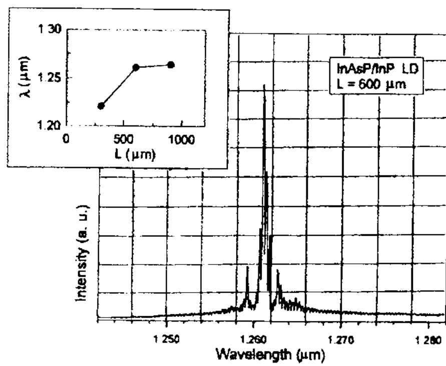

Fig.3 Room-temperature lasing spectrum of a 50 x 600 μm^2 as-cleaved BA LD. The inset shows the relationship between lasing wavelength and cavity length.

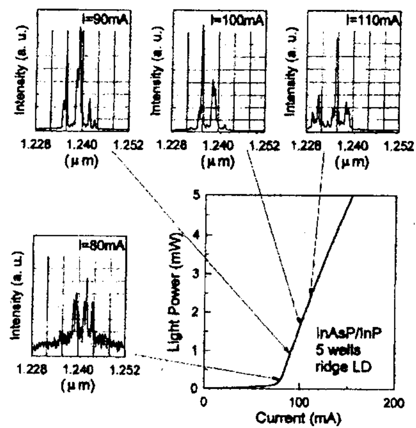

Fig.4 Pulsed light-current characteristics of a 2 x 300 μm^2 as-cleaved RWG LD at room temperature. The lasing spectra at different current levels from 80 to 110 mA are also plotted.